Creep and Stress Relaxation of Granular Materials Simulated by Non-Linear Three-Component Model

Fumio TATSUOKA [a,1] Antoine DUTTINE [b], Alice SALOTTI [c], and Alan EZAOUI [d]
[a] *Department of Civil Engineering, Tokyo University of Science, Japan*
[b] *Integrated Geotechnology Institute Limited, Tokyo, Japan*
[c] *TPC Progretti, Padova, Italy*
[d] *Laboratoire Regional des Ponts & Chaussees, Lyon, France*

Abstract. Creep deformation and stress relaxation during otherwise monotonic loading drained direct shear (DS) at a fixed shear displacement rate of three types of clean sand and a gravel having different particle shapes and exhibiting different viscous property types are simulated by the non-linear three component model. Elastic body represents the hypo-elastic property, plastic body represents the plastic properties exhibiting a non-linear inviscid stress - irreversible strain relation and viscous body represents the viscous properties as a function of irreversible strain and its rate with or without control of loading history. It is shown that the trends of rate-dependent behavior observed in the DS tests, particularly creep and stress relaxation and their relationship, can be successfully simulated in the consistent manner by the non-linear three-component model.

Keywords. creep, direct shear, granular material, simulation, stress relaxation, three-component model

1. Introduction

It is shown in the companion paper (Duttine et al., 2015) that, in drained direct (DS) tests, unbound granular materials (GMs) (i.e., sands & gravels) exhibit "creep and stress relaxation (SR) envelopes" that represent the shear stress - shear displacement states reached by a series of creep and SR for a certain duration starting from different stress states along the same monotonic loading (ML) shear stress - shear displacement curve. The SR envelope is located largely below the creep envelope. Moreover, GMs having different particle shapes and grading characteristics exhibit different viscous property types (i.e., Isotach, Combined, TESRA and P&N), as illustrated in Fig. 1 of the companion paper. As the viscous property type changes from Isotach toward P&N, both creep deformation and stress drop during SR decrease while the decrease in the creep deformation is more significant and the SR envelope is located below the creep envelope more significantly. In this paper, it is shown that these trends of rate-dependent behavior can be simulated very well by the three-component model.

[1] Corresponding Author. Professor, Department of Civil Engineering, Tokyo University of Science, 2641, Yamazaki, Noda City, Chiba Prefecture, Japan; E-mail: tatsuoka@rs.noda.tus.ac.jp

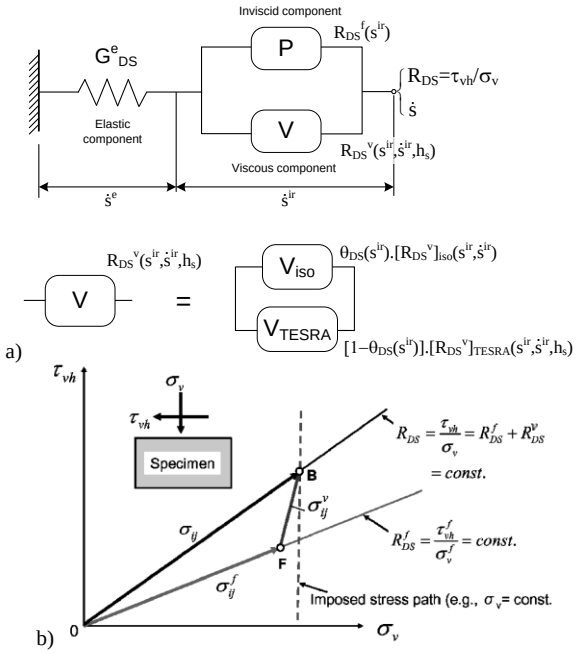

Figure 1. a) Non-linear three-component model adapted to the DS test conditions (h_s: history parameter); and b) relevant stress parameters on τ_{vh}- σ_v plane (Duttine & Tatsuoka, 2009).

2. Non-linear three-component model and model parameters

It has been shown that the three-component model can simulate a wide variety of rate-dependent stress-strain behaviour including creep and SR of geomaterials observed in the triaxial and plane strain compression tests (Di Benedetto et al., 2002; Tatsuoka et al., 2002, 2008) and in the drained DS tests (Tatsuoka et al., 2008; Kongkitkul et al., 2008; Duttine et al. 2009: Duttine & Tatsuoka. 2009). Fig. 1 shows this model adapted to the DS test condition. The shear displacement rate ($\dot{s}$) comprises elastic part ($\dot{s}^{e}$) and irreversible (or visco-plastic) part ($\dot{s}^{ir}$). In this study, it is assumed that the tangent elastic modulus G^{e}_{DS} of the R_{DS} - s^{e} relation of Elastic component is constant in the respective DS tests. The value of G^{e}_{DS} in each test was determined by performing small unload/reload tests during otherwise ML. The shear stress ratio (R_{DS}) comprises inviscid part (R_{DS}^{f}) in *P* body and viscous part (R_{DS}^{v}) d in *V* body. R_{DS}^{v} is expressed as:

$$R_{DS}^{v}(s^{ir},\dot{s}^{ir},h_s)=\theta_{DS}(s^{ir})\cdot\left[R_{DS}^{v}\right]_{iso}(s^{ir},\dot{s}^{ir})+\left[1-\theta_{DS}(s^{ir})\right]\cdot\left[R_{DS}^{v}\right]_{TESRA}(s^{ir},\dot{s}^{ir},h_s) \quad (1)$$

where h_s is the history parameter; and θ_{DS} is the DS viscous property type parameter that characterizes the different viscous property types: i.e., θ_{DS}= 1.0 with Isotach type (in this case, R_{DS}^{v} becomes Isotach viscous stress, $[R_{DS}^{v}]_{iso}$); 0 <θ_{DS}< 1.0 with Combined type; θ_{DS}= 0 with TESRA type (in this case, R_{DS}^{v} becomes TESRA viscous stress, $[R_{DS}^{v}]_{TESTA}$); and θ_{DS}< 0 with P&N. $[R_{DS}^{v}]_{iso}$ and $[R_{DS}^{v}]_{TESTA}$ are obtained as:

$$\left[R_{DS}^{v}\right]_{iso}(s^{ir},\dot{s}^{ir}) = R_{DS}^{f}(s^{ir})\cdot g_{v}(\dot{s}^{ir}) = R_{DS}^{f}(s^{ir})\cdot\alpha\cdot\left\{1-\exp\left[1-(\frac{\left|\dot{s}^{ir}\right|}{\dot{s}_{ref}^{ir}}+1)^{m}\right]\right\} \quad (2a)$$

$$\left[R_{DS}^{v}\right]_{TESRA}(s^{ir},\dot{s}^{ir},h_{s}) = \int_{\tau=a}^{\varepsilon^{ir}}\left[dR_{DS}^{v}\right]_{iso(\tau)}\cdot g_{decay}(s^{ir}-\tau) = \int_{\tau=a}^{\varepsilon^{ir}}\left[dR_{DS}^{v}\right]_{iso(\tau)}\cdot r_{1}^{(s^{ir}-\tau)} \quad (2b)$$

where R_{DS}^{f} is the inviscid stress ratio. The reference relation in terms of the R_{DS}^{f} - s ($=s^{e}+s^{ir}$) relation in the respective DS tests was determined by fitting the test data to:

$$R_{DS}^{f}(s^{ir}) = \left(\frac{2\sqrt{s_{p}.s^{ir}}}{s_{p}+s^{ir}}\right)^{a}.R_{p}\cdot\left(\frac{1}{1+e^{-2.k.s^{ir}}}-\frac{1}{1+e^{-2.k.(s^{ir}-s_{p})}}\right)+\frac{R_{r}+(R_{p}-R_{r}).e^{-\left(\frac{\left|s^{ir}-s_{p}\right|}{s_{r}}\right)^{2}}}{1+e^{-2.k.(s^{ir}-s_{p})}} \quad (3)$$

where R_{p} and R_{r} are the peak and residual values of R_{DS}^{f}; $s^{ir}= s - s^{e}$ ($= R_{DS}/G_{DS}^{e}$); s_{p} and s_{r} are the values of s^{ir} at the peak stress state and the start of residual state; a (> 0) is a constant; and k is another constant controlling the transition from the first term in the pre-peak regime toward the second terms in the post-peak regimes. The value of k is equal to 100 for dense specimens and 50 to 60 for loose to medium-dense specimens.

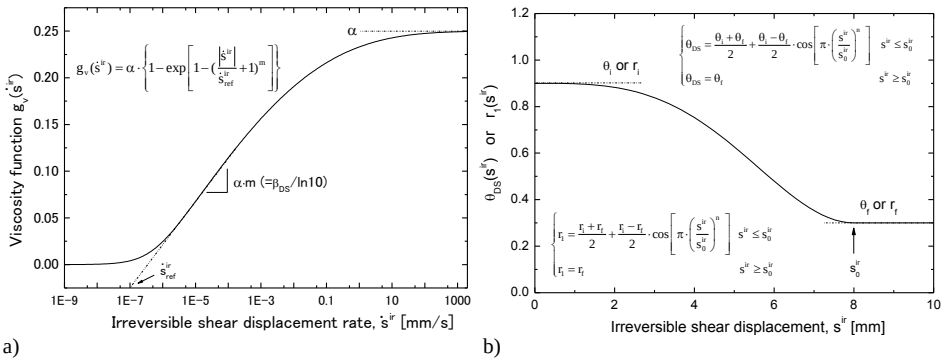

a) b)

Figure 2. a) g_{v}; and b) θ_{DS} & r_{1} as a function of s^{ir} used in the simulation in this study.

$g_{v}(\dot{s}^{ir})$ in Eq. 2a is the viscosity function that is a non-linear function of $\dot{s}^{ir}$ (Fig. 2a). The method to determine the parameters {α; m; $\dot{s}_{ref}^{ir}$ } of this function is explained later. $g_{\text{decay}}= r_{1}^{(s^{ir}-\tau)}$ in Eq. 2b is the decay function, where r_{1} is the decay parameter (< 1.0). r_{1} controls the decay rate of $[dR_{DS}^{v}]_{iso}$ that takes place when $s^{ir} = \tau$ with an increase in s^{ir} during subsequent loading. When $r_{1}= 1.0$ therefore, $r_{1}^{(s^{ir}-\tau)} = 1.0$, $[dR_{DS}^{v}]_{iso}$ does not decay and $[R_{DS}^{v}]_{TESRA}$ (Eq. 2b) becomes $[R_{DS}^{v}]_{iso}$ (Eq. 2a). When $0 < r_{1} < 1.0$, $[dR_{DS}^{v}]_{iso}$ decays at a rate that increases with a decrease in r_{1}. In this case, $[R_{DS}^{v}]_{TESRA}$ (Eq. 2b) could be either positive or zero or negative depending on loading history. The direct integration of Eq. 2b for a given full previous loading history in a numerical simulation (e.g., FEM analysis) of a boundary value problem is extremely time-consuming, thus not practical. This integration becomes practical by using an equation in an incremental form derived from Eq. 2b by taking advantage of the nature of the power law of the

decay function (Tatsuoka et al., 2008; Duttine & Tatsuoka, 2009; Kongkitkul et al., 2008). θ_{DS} and r_1 decrease with s^{ir} as illustrated in Fig. 2b, where $\{\theta_i; r_i\}$ and $\{\theta_f; r_f\}$ are respectively the initial and final values of θ_{DS} and r_1; and $\{n;\ s_0^{ir}\}$ are constants. Duttine and Tatsuoka (2009) showed a strong correlation between θ_{DS} and r_1 with a large variety of poorly-graded granular materials.

The parameters $\{\alpha;\ m;\ \dot{s}_{ref}^{ir}\}$ of the viscosity function, g_v (Fig. 2a), were determined as follows. As the present study does not deal with the behaviour at extremely high shear displacement rates, it is not necessary to accurately determine the value of α. So, α= 0.25 was assumed. On the other hand, the value of m was determined so that the slope of the linear part of the g_v – log($\dot{s}^{ir}$) relation (Fig. 2a), which is theoretically equal to $\alpha \cdot m$, becomes equal to β_{DS}/ln(10), where β_{DS} is the rate-sensitivity coefficient defined as $[\Delta R_{DS}/R_{DS}]/\log\left(\dot{s}_{after}^{ir}/\dot{s}_{before}^{ir}\right)$ (Duttine et al., 2009, Duttine and Tatsuoka, 2009). As shown in Fig. 4, ΔR_{DS} is the change in R_{DS}= τ_{vh}/σ_v upon a step change in $\dot{s}^{ir}$ from $\dot{s}_{before}^{ir}$ to $\dot{s}_{after}^{ir}$ during otherwise ML at a constant shear displacement rate. The parameters of g_v used in the simulation presented here are listed in Table 1.

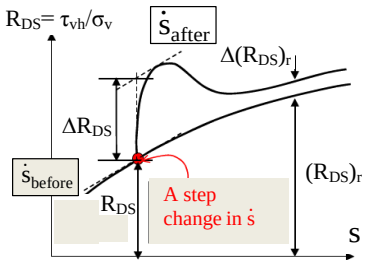

	α	m	$\dot{s}_{ref}^{ir}$ (mm/s)	r_i (i)	r_f (i)
Chiba gravel-a D	0.25	0.035	$2.5\cdot10^{-7}$	10^{-5}	10^{-10}
Chiba gravel-a L	0.25	0.034	$2.5\cdot10^{-7}$	10^{-5}	10^{-10}
Toyoura D	0.25	0.025	10^{-9}	10^{-15}	10^{-25}
Toyoura L	0.25	0.025	10^{-9}	10^{-15}	10^{-25}
Ticino D	0.25	0.026	$5\cdot10^{-7}$	10^{-15}	10^{-25}
Ticino L	0.25	0.024	$5\cdot10^{-8}$	10^{-15}	10^{-25}
Albany D	0.25	0.019	10^{-9}	10^{-25}	10^{-35}
Albany L	0.25	0.027	10^{-9}	10^{-25}	10^{-35}

(i) for shear displacements (s) in mm.

Figure 4 (left). Definitions of β_{DS} & $(\beta_{DS})_r$ (after Duttine et al., 2008, 2009).

Table 1 (right) Parameters for viscosity function, g_v, and decay parameters (D: dense, L: loose)

Table 2. Viscous property type parameter (D: dense, L: loose)

Materials	β_{DS}		$(\beta_{DS})_r$			θ_{DS}			$(\beta_{DS})_r$; θ_{DS}	
	mean(i)	s.d.(ii)	β_i	β_f	s.d.(ii)	θ_i	θ_f	s.d.(ii)	s_0^{ir} (mm)	n
Chiba gravel-a D*	0.0184	0.0022	0.0094	0.001	0.0029	0.51	0.03	0.147	10.5	2.0
Chiba gravel-a L	0.0188	0.0044	0.0094	0.0018	0.0019	0.50	0.05	0.081	6.5	1.5
Toyoura D*	0.0134	0.0011	0	-0.0076	0.0018	0	-0.54	0.167	2.4	1.556
Toyoura L*	0.0135	0.0017	0	-0.0080	0.0012	0	-0.595	0.132	1.25	1.5
Ticino D*	0.0139	0.0018	0	-0.0090	0.0012	0	-0.657	0.103	6.603	3.377
Ticino L	0.0132	0.0021	0	-0.0055	0.0013	0	-0.44	0.106	4.44	0.9
Albany D*	0.0097	0.0016	-0.0030	-0.0135	0.0026	-0.30	-1.40	0.264	1.1	1.0
Albany L	0.0138	0.0028	-0.0194	-0.0194	0.0030	-1.321	-1.321	0.212	--	--

* After Duttine and Tatsuoka (2009) (i) arithmetic.

(ii) Standard deviation $s.d. = 1/\sqrt{N}\cdot\sqrt{\sum_{i=1}^{N}\left[y_i - f(x_i)\right]^2}$ where N is the number of data sets $(x_i; y_i)_{1\le i\le N}$ and $f(x_i)$ is the fitt function (such as Eq. 4) evaluated in $\dot{s}_i^{ir}$.

The parameters $\{\theta_i; r_i;\ \theta_f; r_f;\ n;\ s_0^{ir}\}$ of the viscous property type parameter, θ_{DS} (Fig. 2b), were determined as follows. θ_{DS} is defined as $(\beta_{DS})_r/\beta_{DS}$, where $(\beta_{DS})_r$ is the

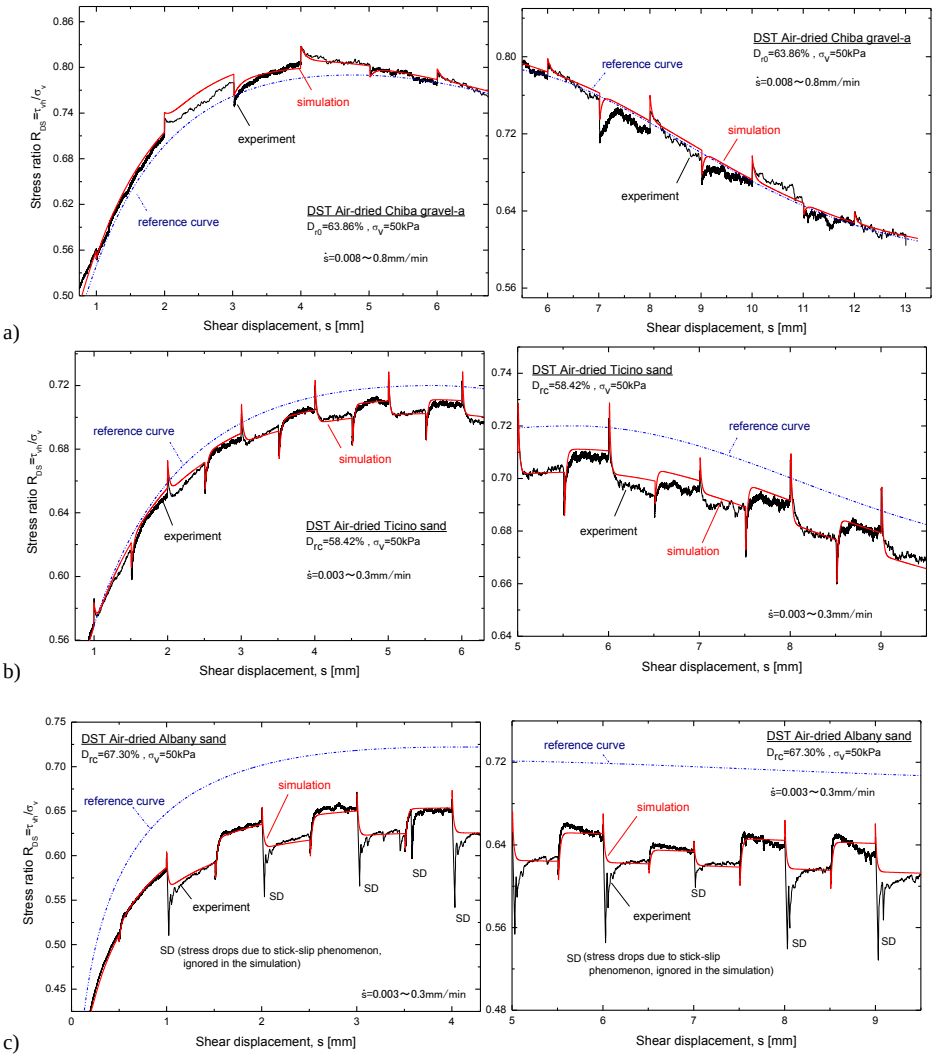

Figure 5. DS tests including step changes in the shear displacement rate in the pre-peak and post-peak regimes and their simulations: a) loose Chiba gravel-a; b) loose Ticino sand; and c) loose Albany sand.

residual value of β_{DS}, defined as $\Delta(R_{DS})_r/(R_{DS})_r/\log\left(\dot{s}^{ir}_{after}/\dot{s}^{ir}_{before}\right)$. As shown in Fig. 4, $\Delta(R_{DS})_r$ is the value of ΔR_{DS} that has fully decayed during the subsequent ML after a step change in $\dot{s}^{ir}$; and $(R_{DS})_r$ is the R_{DS} value at the shear displacement at which $\Delta(R_{DS})_r$ is defined along the stress-displacement curve obtained if ML had continued at the previous $\dot{s}^{ir}$, $\dot{s}^{ir}_{before}$. That is, $(\beta_{DS})_r$ shows how ΔR_{DS} that has taken place by a step change in $\dot{s}^{ir}$ survives subsequent shear displacements. Fig. 5 show typical measured R_{DS} - s relations from DS tests in which the shear displacement rate ($\dot{s}$) was suddenly changed by a factor of 10 or 100 at every shear displacement increment of 0.5 mm or 1.0 mm on loose specimens of three types of GM. The test method is described in details in Duttine et al. (2008). The values of β_{DS}, $(\beta_{DS})_r$ and θ_{DS}, hence the values of

the parameters (m; θ_i; θ_f; n; s_0^{ir}), evaluated by such tests as presented in Fig. 5 are listed in Table 2.

It was confirmed by sieving the test materials before and after the respective tests presented in this paper and the companion paper (Duttine et al., 2015) that crushing of particles in these DS tests was not noticeable. Therefore, the trends of rate-dependent behaviour presented in this paper and the companion papers are not dominantly associated with crushing of particles.

3. Results of simulation

By comparing the test results presented in Fig. 5 with the characteristic features upon a step change in $\dot{s}$ for different viscous property types illustrated in Fig. 1a of the companion paper, it may be seen that these GMs exhibit different viscous property types and different trends of its change with s. That is, in the pre-peak regime, the viscous property type is Combined with Chiba gravel–a (Fig. 5a); TESRA with Ticino sand (Fig. 5b) (and also with Toyoura sand, Duttine & Tatsuoka, 2009); and P&N with Albany sand (Fig. 5c). In the post-peak regime, these viscous property types gradually

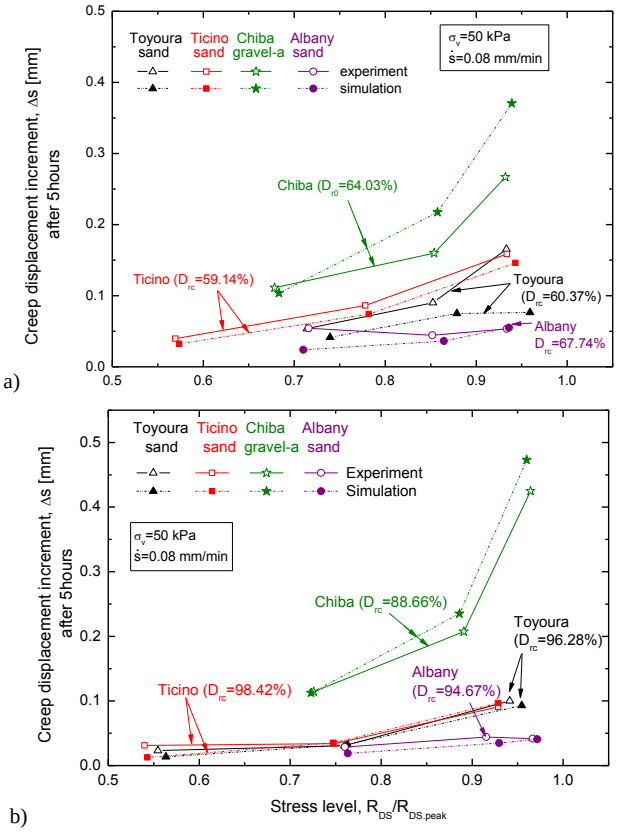

Figure 6. Creep shear displacement after five hours as a function of stress level during otherwise ML (ds/dt= 0.08 mm/min) and their simulations: a) loose; and b) dense granular materials.

change with an increase in *s* toward, respectively, TESRA with Chiba gravel-a; P&N with Ticino sand (and Toyoura sand); and P&N coupled with stick-slip phenomenon with Albany sand. It may also be seen from Fig. 5 that these trends are simulated very well.

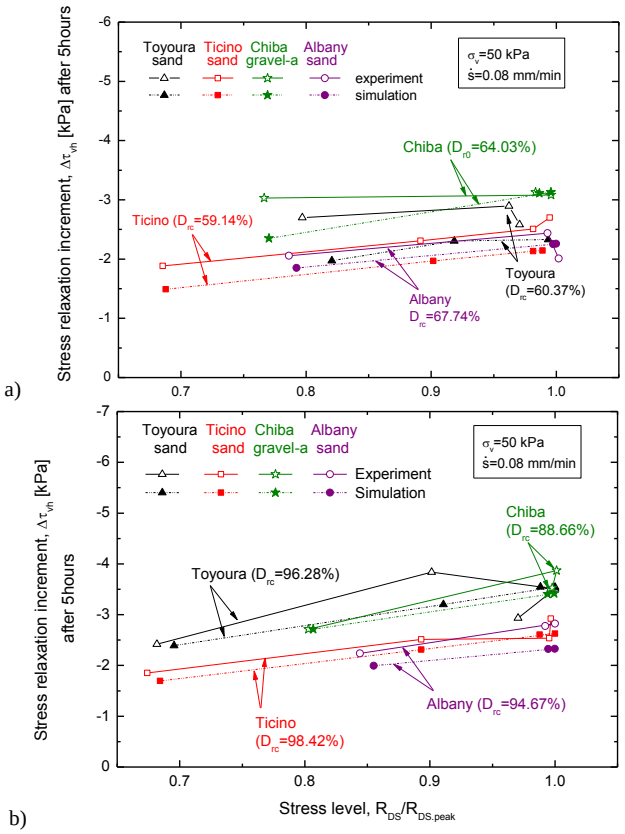

Figure 7. Stress relaxation after five hours as a function of stress level during otherwise ML (ds/dt= 0.08 mm/min) and their simulations: a) loose; and b) dense granular materials.

It may also be seen from Fig. 4, 5 and 6 of the companion paper that the creep and SR behaviours are simulated very well by the model. **Figs. 6a** & **b** compare the experimentally obtained and simulated creep shear displacement after 5 hours as a function of the shear stress level, $R_{DS}/R_{DS.peak}$, where $R_{DS.peak}$ is the measured or simulated peak stress ratio, of loose and dense specimens of four types of GMs exhibiting different viscous property types. Corresponding to the above, **Figs. 7a** & **b** compare the experimentally obtained and simulated stress relaxation after 5 hours as a function of $R_{DS}/R_{DS.peak}$, where R_{DS} is the value at the start of SR in the respective SL tests. It may be seen from Fig. 6 that the effects of shear stress level and specimen density on the creep deformation are significant. On the other hand, the effects of the initial shear stress level on the stress drop during SR are much smaller. This trend is due to that, unlike the creep process, the shear stress level consistently drops during a given SR process, therefore, the effects of initial shear stress become smaller. In addition, the effects of particle shape and the coefficient of uniformity (i.e., the effects

of viscosity property type) on the creep behaviour are significant: i.e., the creep deformation noticeably decreases as the viscous property type becomes less Isotach. On the other hand, the effects of viscous property type on the SR stress drop are smaller. These trends of behaviour observed in the tests are well simulated.

4. Conclusions

The following features of the viscous responses observed in drained direct shear tests can be very well simulated by the three-component model using the same model parameters for the same GM type: a) a stress jump upon a step increase or decrease in the shear displacement rate and their decay at different rates during subsequent monotonic loading (ML) at a constant shear displacement rate; b) a transition of viscous property type with shear displacement; c) the development of a high stiffness zone upon the restart of ML at a constant strain rate from the end of creep or stress relaxation (SR) stage, followed by overshooting of the ML curve; and d) an increase in the creep deformation and the stress drop during SR with an increase in the shear stress level. Moreover, the following trends can be simulated very well. Irrespective of viscous property type (i.e., Isotach, Combined, TESRA and P&N), the SR envelope reached by a series of SR for a certain period that have started from different shear stresses along the same ML shear stress – shear displacement curve is located consistently lower than the corresponding creep envelope obtained under otherwise the same condition. In addition, the effects of viscous property type on the amount and rate of creep deformation and stress drop during SR can be simulated very well.

These results indicate that, when the model parameters are determined appropriately, the three-component model can predict the histories of stresses and/or deformation along arbitrary stress or strain paths, including the creep and SR paths.

References

[1] Di Benedetto, H., Tatsuoka, F. and Ishihara, M., Time-dependent shear deformation characteristics of sand and their constitutive modelling, *Soils and Foundations*, **42**(2) (2002), 1-22.

[2] Duttine, A., Tatsuoka, F., Kongkitkul, W. and Hirakawa, D., Viscous behaviour of unbound granular materials in direct shear, *Soils and Foundations*, **48**(3) (2008), 297-318.

[3] Duttine, A., Tatsuoka, F., Lee, J. and Kongkitkul, W., Viscous properties of Toyoura sand over a wide range of strain rate and its model simulation, *Soils and Foundations*, **49**(2) (2009), 221-247.

[4] Duttine, A. and Tatsuoka, F., Viscous properties of granular materials having different particle shape in direct shear", *Soils and Foundations*, **49**(5) (2009), 777-796.

[5] Duttine, A., Tatsuoka, F., Salotti, A. and Ezaoui, A., Creep and stress relaxation envelopes of granular materials in direct shear, *Proc. of 15th Pan-American Conference on Soil Mechanics and Geotechnical Engineering and 6th International Conference on Deformation Characteristics of Geomaterials, Buenos Aires* (2015), this conference.

[6] Kongkitkul, W., Tatsuoka, F., Duttine, A., Kawabe, S., Enomoto, T. and Di Benedetto, H., Modelling and simulation of rate-dependent stress-strain behaviour of geomaterial, *Soils and Foundations*, **48**(2) (2008), 175-194.

[7] Tatsuoka, F., Ishihara, M., Di Benedetto, H. and Kuwano, R., Time-dependent shear deformation characteristics of geomaterials and their simulation, *Soils and Foundations*, **42**(2) (2002), 103-129.

[8] Tatsuoka, F., Di Benedetto, H., Enomoto, T., Kawabe, S. and Kongkitkul, W., Various viscosity types of geomaterial in shear and their mathematical expression, *Soils and Foundations*, **48**(1) (2008), 41-60.

[9] Tatsuoka, F., Laboratory stress-strain tests for developments in geotechnical engineering research and practice, Bishop Lecture, *Proc. 5th Int. Symp. on Deformation Characteristics of Geomaterials*, IS-Seoul 2011 (Chung et al. eds) (2011), 3-50.